Journal of Photochemistry and Photobiology A: Chemistry 218 (2011) 231–238

Contents lists available at ScienceDirect

Journal of Photochemistry and Photobiology A: Chemistry

journal homepage: www.elsevier.com/locate/jphotochem

Photocatalytic properties of rutile nanoparticles obtained via low temperature route from titanate nanotubes

Dmitry V. Bavykin[a,*], Alexander N. Kulak[a], Vitaly V. Shvalagin[b], Natalya S. Andryushina[b], Olexander L. Stroyuk[b]

[a] Materials Engineering and Energy Technology Research Groups, School of Engineering Sciences, University of Southampton, Southampton SO17 1BJ, United Kingdom
[b] Photochemistry Department, Pysarzhevstki Institute of Physical Chemistry, 31 Nauky av., 03028 Kiev, Ukraine

ARTICLE INFO

Article history:
Received 16 September 2010
Received in revised form
19 November 2010
Accepted 12 January 2011
Available online 22 January 2011

Keywords:
Solvothermal synthesis
Reflux
Surface area
Stability
Mechanism
Rutile nanoparticles
Photocatalysis
Hydrogen generation
Advanced oxidation

ABSTRACT

Acid treatment of titanate nanotubes with 0.1 mol dm^{-3} H_2SO_4 results in their transformation into various forms of nanostructured TiO_2, the shape and crystal structure of which depend on the temperature and time of treatment. Such a transformation at 25 °C results in the formation of rutile spheroidal nanoparticles, which are characterized by good crystallinity, high specific surface area (ca 250 m^2 g^{-1} BET) and small average diameter of particles (ca. 3 nm). These particles are also characterized by increased activity in reactions of both photocatalytic generation of hydrogen from alcohol and advanced oxidation of organic species (ethanol). Acid assisted transformation of nanotubes at higher temperatures results in formation of nanostructured anatase/titanate composites with lower photocatalytic activity. The mechanism of transformation and the reasons for increased activity of rutile nanoparticles are discussed.

1. Introduction

The photocatalytic properties of TiO_2 based materials have been thoroughly studied during the last two decades in numerous processes including advanced oxidation, sustainable hydrogen generation and self cleaning coatings [1]. Despite significant developments in the synthesis of active nanostructured photocatalysts in recent years, the search for new cost effective materials, which can offer higher activity and stability in a number of photocatalytic processes, still continues. Recently discovered titanate nanotubes [2] obtained by alkaline hydrothermal treatment of TiO_2 [3] have demonstrated not only unique combinations of physico-chemical [4,5] and structural [6] properties but also the possibility of their utilization in a wide range of applications [7] including catalysis [8,9], photocatalysis [10,11], mesoporous ion-exchange materials [12,13], lithium batteries [14,15], and solar cells [16,17].

Early studies have shown that despite the extended lifetime of trapped photogenerated charge carriers [18] the photocatalytic activity of as-prepared titanate nanotubes is smaller (but not zero) than the activity of standard Degussa P25 catalyst in e.g. a reaction of oxidation of NH_3 [19] and various dyes [20] or decomposition of dimethyl methylphosphonate and diethylsulphide [21] in aqueous suspensions. Such a decreased activity of nanotubes is probably associated with impurities of sodium ions and low crystallinity of the structures stimulating recombination of electron–hole pairs. Most of the attempts to improve the activity of nanotubes can be divided into two groups, namely heat and combined heat/acid treatments. Calcination of protonated titanate nanotubes results in their dehydration [22] at temperatures 140–350 °C followed by transformation of titanate crystal structure to monoclinic TiO_2-(B) at 350 °C [23]. A further increase in the temperature above 450 °C results in collapse of tubular morphology and formation of anatase nanorods at 450 °C, characterized by a photocatalytic activity which is higher than titanate nanotubes [24,25] probably due to better crystallinity. A further increase in calcination temperature resulted in a lower photocatalytic activity due to stripping off the surface –OH groups and reduction in the surface area of nanostructures.

Since nanotubular titanates are produced in alkaline environment, they are thermodynamically unstable in acid environment [26] and undergo slow transformation to nanostructured TiO_2 even at room temperature [27]. The crystal structure, morphology and photocatalytic properties of obtained TiO_2 depend on the nature

* Corresponding author. Tel.: +44 2380598358; fax: +44 2380598754.
E-mail address: D.Bavykin@soton.ac.uk (D.V. Bavykin).

1010-6030/$ – see front matter © 2011 Elsevier B.V. All rights reserved.
doi:10.1016/j.jphotochem.2011.01.006

of the acid and the temperature of the treatment. For example, hydrothermal treatment of nanotubes with residual HCl at 200 °C [28] or nanofibres with 0.1 M HNO_3 (pH 0–7) at 180 °C [29] results in the formation of nanostructured anatase with a fibrous or particulate morphology, which showed higher photocatalytic activity than initial nanostructured titanates.

In this work, the effect of acid treatment of titanate nanotubes with H_2SO_4 at temperatures varied from 25 to 70 °C on their photocatalytic activity in the reaction of ethanol oxidation or hydrogen generation from water/ethanol mixtures has been studied systematically. The activity of catalysts has been correlated with their crystallographic, morphological, and adsorption properties. The unusually high activity of rutile nanoparticles produced by low temperature acid treatment of nanotubes is reported for the first time.

2. Experimental procedure

2.1. Preparation of samples

Sodium hydroxide (NaOH), potassium hydroxide (KOH), hydrochloric acid (HCl), sulphuric acid (H_2SO_4), ethanol and hydrogen peroxide (H_2O_2), pure grade were all obtained from Aldrich and were used without further purification. Titanium dioxide (P25, TiO_2) was obtained from Degussa.

The preparation of titanate nanotubes was based on the alkaline hydrothermal method proposed by Kasuga et al. [3] and further developed in our laboratories towards a lower temperature synthesis using KOH–NaOH mixtures [30] allowing a reflux method to be used rather than an autoclave. 20 g of titanium dioxide was mixed with of 240 cm^3 of 10 mol dm^{-3} NaOH and 10 cm^3 of 10 mol dm^{-3} KOH aqueous solutions, then placed in a PFA (a perfluoroalkoxy polymer) round bottom flask equipped with a thermometer and refluxed at 106 °C for 4 days without stirring. The white, powdery titanate nanotubes produced were thoroughly washed with water until the washing solution achieved pH 7.

For acid treatment, 1 g of obtained titanate nanotubes was placed in 50 cm^3 round bottom flask and mixed with 25 cm^3 of 0.1 mol dm^{-3} H_2SO_4. Samples were treated at 25, 40 and 70 °C without stirring. After a controlled time in the range of 4 days to 3 months, each sample was filtered, washed with water and dried at 25 °C in a vacuum.

2.2. Measurement of isotherm of adsorption

The sample of mass m was placed in the bottle of volume V filled with air and sealed with a stopper. A certain volume of ethanol was injected into the bottle using a micro-syringe. After establishment of adsorption–desorption equilibrium (60 min), the concentration of ethanol (C) in gas phase was measured using Gas Chromatograph Chrom 5. The amount of ethanol adsorbed on the surface of nanostructured materials (a) was calculated using the formula

$$a = \frac{(C^0 - C)V}{m} \quad (1)$$

where C^0 is the concentration of ethanol in gas phase without sample.

2.3. Characterization of photocatalytic activity

The photocatalytic activity of nanostructured samples was measured in both the reaction of oxidation of ethanol vapours and the reaction of hydrogen evolution from ethanol–water mixture. In first case, 50 mg of the sample was wet deposited onto a 3 × 3 cm glass plate and placed in a thermostatic 142 cm^3 batch reactor equipped with a fused silica window, magnetic stirrer for air circulation and a sampling port with membrane. The desired amount of liquid ethanol was injected into the reactor and allowed 2 h for complete evaporation of ethanol and its adsorption on the surface of the catalyst prior to illumination. For photocatalytic hydrogen evolution studies, the sample of nanostructured TiO_2 was mixed with a co-catalyst (2 wt% Pd/SiO_2 KSK-200 with a grain size from 0.25 to 0.5 mm) [31] in a weight ratio 5:1, then 0.05 g of mixture was placed into 10 cm^3 thermostated cylindrical reactor filled with 10 cm^3 ethanol–water mixture (2 vol.% water). In both cases, the samples were illuminated with focused light from a 1000 W high pressure mercury arc lamp (Drsh-1000) filtered using both standard optical and water cut off filters in order to isolate the spectral range from 310 to 390 nm. The intensity of incident light was measured using the ferrioxalate actinometry as 1.37×10^{17} quanta/s at the incident power density of 25 mW/cm^2, measured using the Gentec EO bolometer equipped with PH100-SiUV photodiode. The concentration of ethanol, acetaldehyde, hydrogen, acetic acid and CO_2 was measured using gas chromatography.

2.4. Sample characterization

The BET surface area of the samples was measured, using nitrogen adsorption, on a Micromeritics Gemini 2375 instrument. TEM images were obtained using a JEOL 3010-TEM transmission electron microscope. The powder sample was “dry” deposited onto a copper grid covered with a perforated carbon film. XRD patterns were recorded using DRON-3M X-ray diffractometer equipped with a source of copper K_α irradiation.

3. Results and discussion

A recent approach for improvement of charge separation in semiconductor photocatalysts utilizes a synergetic effect of mixed phase titania nanocomposites in which the small difference in flat band potentials between two crystal forms of TiO_2 (e.g. anatase and rutile) stimulates spatial separation of carriers reducing their recombination rate [32]. Successful charge separation in such mixed phase composites requires development of efficient contact between two phases, which can be adjusted by a synthetic procedure. Versatile chemistry of titanate nanotubes provides a facile route for preparation of mixed phase composites with improved photocatalytic activity. For example, the bi-crystalline mixture of 33% of TiO_2-(B) nanotubes and 67% of anatase nanoparticles prepared by calcination of protonated titanate nanotubes is characterized by an increased photocatalytic activity compared to P25 TiO_2 for hydrogen evolution from aqueous ethanol [33].

Another prospective route for mixed phase composite synthesis is based on the thermodynamic instability of titanates nanotubes suspended in aqueous solutions of inorganic acids, which results in their slow transformation into nanostructured TiO_2 accompanied by the loss of nanotubular morphology [27,34]. The particular shape and crystal structure of obtained TiO_2 nanostructures depend on the concentration of acid, temperature, and the duration of the transformation. The additional advantage of acid assisted transformation in presence of H_2SO_4 is associated with the modification of the surface of TiO_2 nanoparticles resulting in improvements of their photocatalytic activity in advanced oxidation process [35].

Fig. 1 shows TEM images of initial titanate nanotubes and material obtained after their treatment with 0.1 mol dm^{-3} H_2SO_4 at 25 °C for 90 days after which the original titanate nanotubes have completely disappeared and spheroidal nanoparticles of rutile have formed. The initial nanotubes are characterized by a multi-

Table 1
Physico chemical and photocatalytic properties of nanostructured TiO_2 obtained by acid assisted transformation of titanate nanotubes. The values for a_{sat} and k^E_{ads} were determined by fitting adsorption data from Fig. 4 to Eq. (2). The value of C^0_E was measured experimentally. The values of W^0 were determined as the initial slope of the plot (C_E/C^0_E) *vs.* time in Fig. 5 multiplied by the product of C^0_E and the volume of the reactor V. The values of k_1 were estimated using Eq. (3).

N	Method of synthesis	BET ($m^2\,g^{-1}$)	Phases composition from XRD pattern		a_{sat} ($mmol\,g^{-1}$)	k^E_{ads} ($dm^3\,mmol^{-1}$)	C^0_E ($mmol\,dm^{-3}$)	$W^0 \times 10^5$ ($mmol\,min^{-1}$)	$k_1 \times 10^4$ ($g\,min^{-1}$)	Morphology
1	Initial nanotubes	200	100% $H_2Ti_3O_7$		0.617	375	0.110	5.4	0.89	Tubes: 4 nm diameter, 100+ nm length
2	0.1 mol dm^{-3} H_2SO_4 for 14 days at 25 °C	251	≈75% $H_2Ti_3O_7$	≈25% rutile	0.528	380	0.062	10.7	2.11	Impurities of nanoparticles to tubes
3	0.1 mol dm^{-3} H_2SO_4 for 60 days at 25 °C	184	≈5% $H_2Ti_3O_7$	≈95% rutile	0.272	114	0.137	12.0	4.69	Impurities of tubes to nanoparticles
4	0.1 mol dm^{-3} H_2SO_4 for 90 days at 25 °C	246	≈98% rutile	≈2% anatase	0.161	74	0.122	12.7	8.78	Spheroidal nanoparticles ≈3 nm
5	0.1 mol dm^{-3} H_2SO_4 for 4 days at 40 °C	96	≈30% $H_2Ti_3O_7$	≈70% rutile	0.496	240	0.079	7.8	1.65	Elongated rutile nanostructures
6	0.1 mol dm^{-3} H_2SO_4 for 4 days at 70 °C	210	≈90% anatase	≈10% rutile	0.461	90	0.055	11.7	3.05	Spheroidal anatase nanoparticles ≈4 nm
7	Degussa P25	50	≈70% anatase	≈30% rutile	0.292	154	0.084	23.9	8.80	Spheroidal nanoparticles ≈25 nm

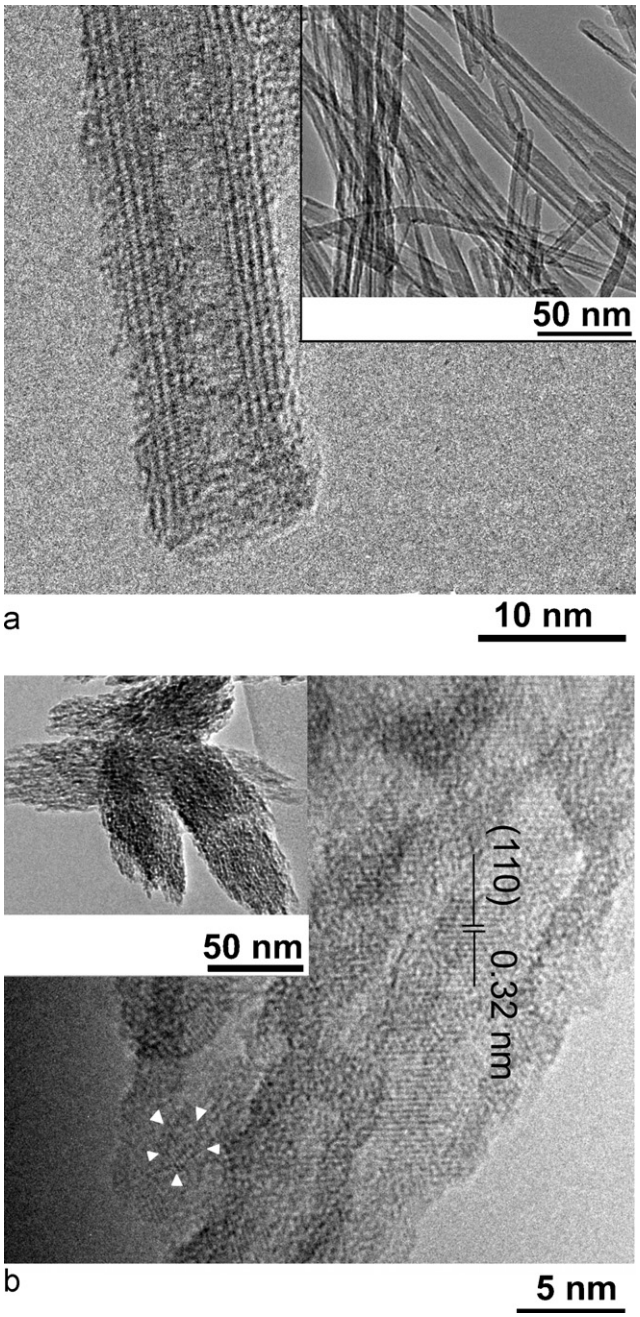

Fig. 1. TEM images of (a) initial titanate nanotubes and (b) rutile nanoparticles obtained by treatment of nanotubes with 0.1 mol dm^{-3} H_2SO_4 for 3 months at 25 °C. Inset shows lower magnification. White arrows indicate the boundary of the particle.

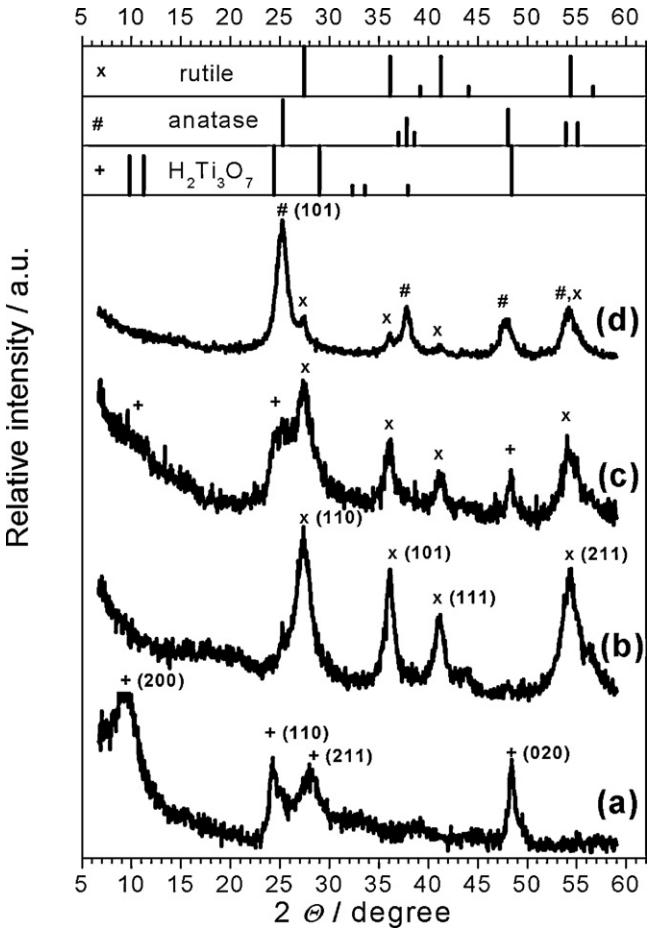

Fig. 2. Powder XRD pattern titanate nanotubes treated with 0.1 mol dm^{-3} H_2SO_4: (a) initial nanotubes, (b) at 25 °C for 90 days, (c) at 40 °C for 4 days, (d) at 70 °C for 4 days. Rutile (x), anatase (#) and $H_2Ti_3O_7$ (+) reflections are shown as line pattern. For most of the peaks the typical value of the detector count was in the range of several hundreds.

layer wall structure with an interlayer spacing of approximately 0.74 nm between (1 0 0) planes in the monoclinic $H_2Ti_3O_7$ [36] observed in XRD pattern as a characteristic reflection at low angles (see Fig. 2a). The average internal diameter of nanotubes is approximately 4 nm and the length exceeds several hundreds of nanometers. In contrast, nanoparticles of TiO_2 obtained after acid treatment at room temperature are characterized by spheroidal shape with an average diameter of the particles of approximately 3 nm. The crystal structure of particles corresponds to a rutile phase (see Fig. 2b) with small impurities of anatase (see Table 1). The particles are agglomerated into elongated structures with typical dimensions of 50 × 200 nm. The ellipsoid shape of the agglomerate is probably associated with elongated geometry of the initial titanate nanotubes. At the early stages of transformation both initial titanate nanotubes and rutile nanoparticles can be found (see Table 1).

The mechanism of acid assisted transformation of titanate nanotubes into nanostructured TiO_2 includes dissolution of nanotubes, release of soluble forms of Ti(IV) in solution, and crystallization of dissolved Ti(IV) to TiO_2 [27]. The steady state concentration of dissolved Ti(IV) and the rate of transformation depend on the nature and concentration of the acid as well as on the temperature of the solution. The morphology and the phase composition of nanostructured TiO_2 are affected by the rate of the process. The rutile nanoparticles tend to form at a low reaction rate whereas nanostructured anatase is usually obtained at elevated rates of the transformations [27,34]. In the intermediate case formation of mixed phase composites is possible.

Fig. 3 shows nanostructured TiO_2 obtained by acid treatment of titanate nanotubes with 0.1 mol dm^{-3} H_2SO_4 at 40 °C and 70 °C for 4 days. The main product of transformation at 40 °C is the elongated rutile nanostructures with impurities of unreacted titanate nanotubes (Fig. 3a). Rutile elongated nanoparticles are agglomerated into ellipsoid shape nanostructures. The phase composition according to TEM and XRD data is a mixture of rutile and trititanate (see Table 1). In contrast, acceleration of the reaction by an increase in temperature results in preferential formation of anatase nanoparticles of spheroidal shape with average diameter ca. 4 nm agglomerated into irregular structures (see Fig. 3b). The phase composition of the product is anatase with impurities of rutile (see

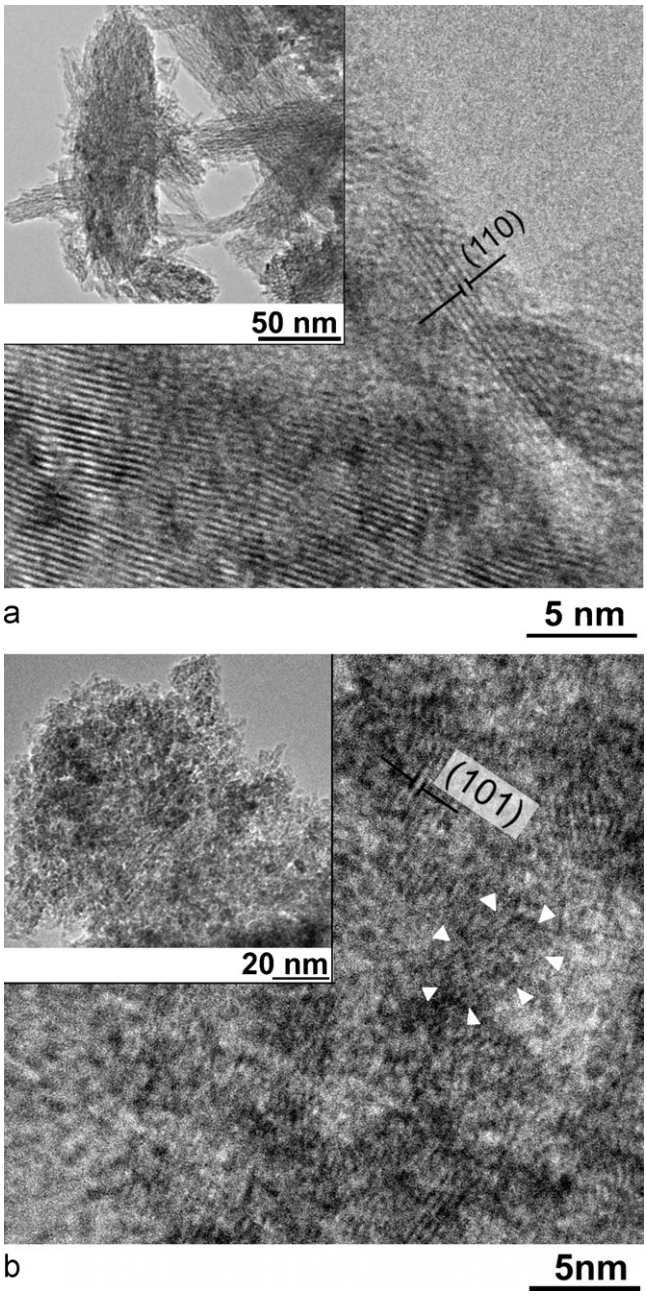

Fig. 3. TEM images of nanostructured TiO_2 and titanates obtained by treatment of titanate nanotubes with 0.1 mol dm^{-3} H_2SO_4 (a) at 40 °C for 4 days and (b) at 70 °C for 4 days. Inset shows lower magnification. White arrows indicate the boundary of the particle.

Table 1). No initial titanate phase is found indicating 100% conversion of the titanate nanotubes into TiO_2 after 4 days.

All products of acid assisted transformation of titanate nanotubes into nanostructures of TiO_2 are characterized by a high specific surface area measured by nitrogen adsorption (see Table 1). Typical values of BET surface area exceed 100 m^2 g^{-1}. However, due to the crystallographic differences, the nature of the surface including surface acidity, density of surface OH groups, zeta potential of particles in aqueous suspension of nanostructured titanates and TiO_2 can vary significantly [2]. As a consequence, the affinity of the nanostructured titanates and TiO_2 towards organic molecules can also vary to a large extent. Fig. 4 shows isotherms of ethanol adsorption in the surface of nanostructured TiO_2 and titanate nanotubes at 25 °C from air. The curves can be approximated by the Langmuir

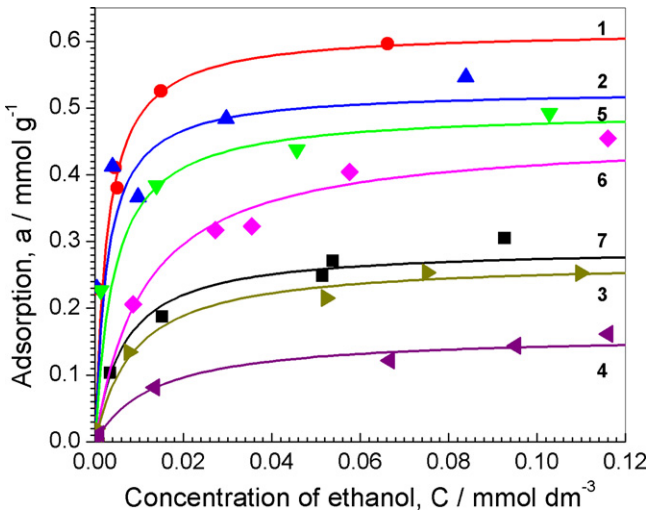

Fig. 4. Isotherms of ethanol adsorption from gas phase (air) on the surface of nanostructured TiO_2 at 25 °C. (1) Is initial titanate nanotubes. (2–4) Are rutile titanate/rutile mixture obtained by treatment of nanotubes with 0.1 mol dm^{-3} H_2SO_4 at 25 °C for 14 days, 60 days and 90 days respectively. Samples (5) and (6) were obtained by treatment with 0.1 mol dm^{-3} H_2SO_4 for 4 days at 40 °C and 70 °C respectively. (7) Is P25 standard. All fitting curves were obtained by fitting data points to Eq. (2).

adsorption equation

$$a = \frac{a_{sat} K^{E}_{ads} C_E}{1 + K^{E}_{ads} C_E} \quad (2)$$

where a_{sat} corresponds to the amount of ethanol forming a monolayer on the surface of adsorbent (mol g^{-1}) and k^{E}_{ads} is the constant of adsorption of ethanol (dm^3 mol^{-1}), C_E is the concentration of ethanol in gas phase (mol dm^{-3}). For most of the samples when concentration of ethanol in the air exceeds 0.1 mmol dm^{-3} the surface of nanotubes and nanoparticles becomes saturated with adsorbed molecules of ethanol. Values of the adsorption constant (k^{E}_{ads}) and saturation concentration (a_{sat}) for titanate nanotubes and nanostructured TiO_2, estimated by fitting the data from Fig. 4 to Eq. (2), are shown in Table 1. It is remarkable that acid assisted transformation of titanate nanotubes to rutile or anatase nanoparticles results in a considerable decrease in both K_{ads} and a_{sat} values. Taking into account that the value of specific surface area of titanate nanotubes is similar to that of rutile nanoparticles obtained after 90 days acid treatment at 25 °C (see Table 1), such a decrease in a_{sat} can be explained by dramatic modification of the surface nature resulting in lowering of the amount of adsorption sites. Usually, transformation of titanate nanotubes into nanostructured TiO_2 is also accompanied by significant (but not to zero) decrease in the density of surface ion-exchangeable –OH groups [22], which are probably associated with adsorption sites for ethanol. Modification of the surface also decreases its affinity to ethanol molecules by lowering the interaction energy between adsorbate and adsorbent and decreasing the adsorption constant K_{ads}.

Such a difference in adsorption properties of the samples can affect significantly the apparent kinetics of photocatalytic oxidation of ethanol vapours on their surface, mechanism of which has been thoroughly studied and showed formation of several principal intermediates in the gas phase [37,38]. The kinetic rate of ethanol degradation using TiO_2 photocatalysts usually can be described [39] using Langmuir–Hinshelwood expression:

$$W = \frac{k_1 a_{sat} K^{E}_{ads} C_E}{1 + K^{E}_{ads} C_E + K^{A}_{ads} C_A + K^{F}_{ads} C_F} \quad (3)$$

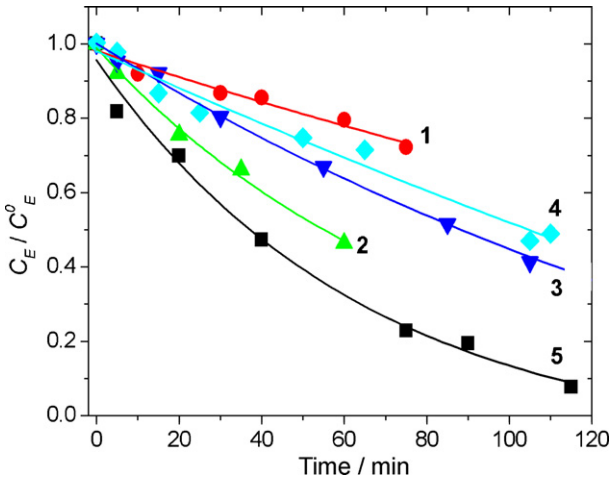

Fig. 5. Kinetic curves of photocatalytic oxidation ethanol on the surface of (1) initial titanate nanotubes, (2–4) titanate/rutile mixed nanostructures obtained by treatment of nanotubes with 0.1 mol dm^{-3} H_2SO_4 at 25 °C for 14 days, 60 days and 90 days respectively and (5) P25 standard reference. Initial concentration of ethanol in gas phase C^0_E varies between 0.133 and 0.055 mmol dm^{-3} (see Table 1). Mass of photocatalyst is ca. 50 mg. The intensity of incident light (310 nm < λ < 380 nm) is 1.37×10^{17} quanta/s. Temperature is 25 °C. Relative humidity is ca. 70%.

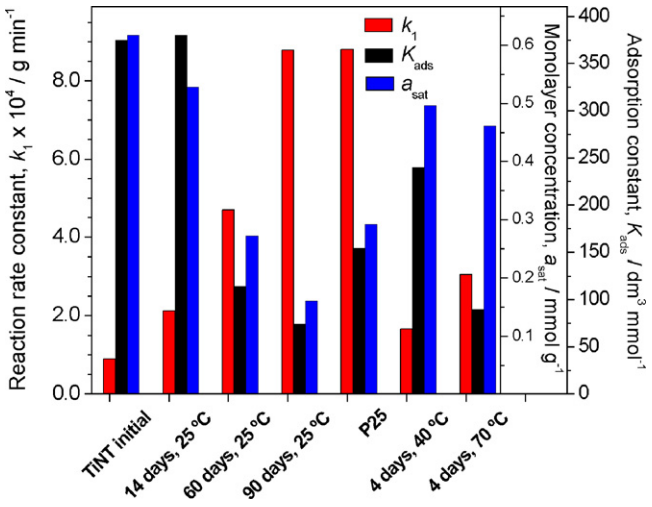

Fig. 6. The rate constant of photocatalytic oxidation of ethanol vapours (k_1) and Langmuir adsorption constant (K_{ads}) of ethanol on the surface of nanostructured TiO_2 obtained by treatment of titanate nanotubes (TiNT) with 0.1 mol dm^{-3} H_2SO_4.

where W is the ethanol oxidation rate per volume of illuminated catalyst, k_1 is the photocatalytic reaction rate constant, C_i and k^i_{ads} are the concentration and binding adsorption constant of the i component (E = ethanol, A = acetaldehyde, F = formaldehyde). Eq. (3) is validated only under assumptions that the background concentration of oxygen is constant and the final product CO_2 does not inhibit photocatalytic process. Large variation in both K^i_{ads} and a_{sat} for different samples obtained by acid treatment of titanate nanotubes can complicate comparison of their photocatalytic activity. In order to accurately compare activity of nanostructured TiO_2 and titanates, the rate constant of photocatalytic oxidation, k_1 can be calculated using Eq. (3) and used as a comparison parameter. Additional simplifications can be achieved by measuring the initial rate of ethanol oxidation, when $C_A = 0$ and $C_F = 0$ and surface coverage by acetaldehyde and formaldehyde is negligible.

In order to study the activity of nanostructured TiO_2 and titanate in the reaction of photocatalytic oxidation of ethanol vapours, the choice of experimental conditions had to satisfy the following requirements. The concentration of ethanol in gas phase before irradiation but after adsorption on the surface of catalyst (C^0_E) was selected to be approximately 0.1 mmol dm^{-3} allowing the reaction to proceed on the ethanol-saturated surface of the photocatalyst (see Fig. 4) and resulting in the apparent zero order kinetics of ethanol degradation. The required amount of injected ethanol (ν^E) was calculated using the equation

$$\nu^E = C^0_E V + \frac{a_{sat} K^E_{ads} C^0_E m}{1 + K^E_{ads} C^0_E} \quad (4)$$

where V is the volume of the reactor and m is the mass of catalyst. The parameters K^E_{ads} and a_{sat} for each sample were estimated from adsorption experiments (Table 1). All samples had similar mass were illuminated with the same intensity of light. The oxygen was in excess in order to neglect the decrease of its concentration during the reaction.

Fig. 5 shows kinetic curves of photocatalytic degradation of ethanol on the surface of nanostructured TiO_2 obtained via acid transformation of titanate nanotubes. Photocatalytic oxidation of ethanol is accompanied by the release of intermediate acetaldehyde and finally CO_2 (data are not shown here). For most of the samples, except for P25, the kinetic curves of ethanol oxidation follow a linear relationship with time, indicating the saturation of the catalyst surface with ethanol at least during first 40 min of the reaction. This has allowed accurate measurements of the initial rate of ethanol decomposition W^0 (see Table 1), determined as the initial slope of the plot (C_E/C^0_E) *vs.* time multiplied by the product of C^0_E and the volume of the reactor V. Although the amount of injected ethanol into the reactor was calculated using Eq. (4), the resulting concentration of ethanol in the gas phase after adsorption and before illumination C^0_E varied between 0.137 and 0.055 mmol dm^{-3} (see Table 1) due to the experimental error of determination of K^E_{ads} and a_{sat} parameters.

The values of W^0, K^E_{ads} and a_{sat} allow us to determine the apparent rate constant of photocatalytic oxidation of ethanol on nanostructured TiO_2 (k_1) using Eq. (3). For this calculation it is assumed that K^E_{ads} and a_{sat} determined in the dark conditions can be applied to Eq. (3), which consider these values under illumination. This assumption, however, still can be applied as was shown elsewhere [40]. The resulting values of k_1 are shown in Table 1 and Fig. 6. The rutile nanoparticles obtained at 25 °C after 90 days treatment are characterized by a high value of k_1, which is slightly higher than that for P25. Such an increased value of reaction rate constant can be associated with the small size of nanoparticles together with their good crystallinity, providing efficient collection of photogenerated carriers by their surface and improving the quantum yield of the photocatalytic reaction. An additional factor contributing to overall good performance of rutile nanoparticles can be also associated with their poor adsorption properties, leading potentially to efficient desorption of the products of ethanol oxidation, thus unblocking the surface of the photocatalyst. Besides, observed impurities of anatase phase (~2%) can also stimulate efficient charge separation of photogenerated carriers in anatase/rutile interface [32] decreasing the rate of their recombination. Overall performance of such rutile nanoparticles, however, is still lower than that for P25 due to the low value of ethanol monolayer density and adsorption constant.

The comparison of the sample 3 with 4 (Table 1) shows that insignificant rise in rutile content from 95% to 98%, accompanied by disappearance of initial titanate and appearance of anatase impurities result in an increase of reaction rate k_1 as well as the small rise of the specific surface area of the sample. At the same time, both ethanol adsorption constant K^E_{ads} and monolayer density a_{sat} are decreasing. Such spontaneous change of many parameters indicates considerable change in the nature of the surface of nanostructured TiO_2 materials.

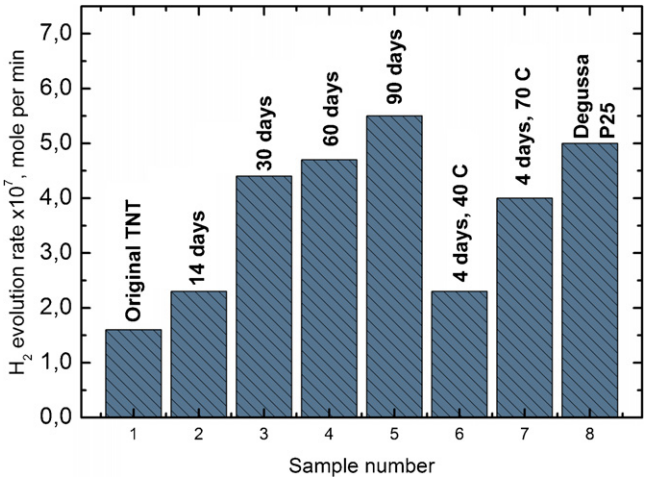

Fig. 7. The rate of hydrogen evolution from ethanol:water (98:2, v/v) mixture using of nanostructured TiO_2 catalyst obtained by treatment of titanate nanotubes (TiNT) with 0.1 mol dm^{-3} H_2SO_4.

Catalysts obtained by acid treatment under elevated temperatures are also characterized by increased photocatalytic activity relative to the initial titanate nanotubes (see samples 5 and 6 in Table 1). However, no strong effect of mixed phases on the improvements associated with effective charge separation in the interface can be detected. Although HRTEM data shows good interface between different phases (anatase/rutile) (see e.g. Fig. 3), the photocatalytic activity of such samples cannot be unambiguously interpreted to confirm the beneficial effect of mixed phase improvement. The difficulties in interpretation of the photocatalytic data are linked to several effects simultaneously occurring during the acid assisted transformation of titanate nanotubes and affecting the activity of photocatalysts. These are formation of a new crystal phase (anatase or rutile), accompanied by a modification of the surface properties of samples, including specific area and affinity for organic molecules. Further optimisation of the acid treatment of titanate nanotubes, however, may potentially lead to formation of mix phase nanostructured composites with optimal surface properties for high photocatalytic activity.

Preliminary studies have shown that the anaerobic irradiation with UV light of nanostructured TiO_2 and titanate nanotubes suspended in water–alcohol mixture in the presence of Pd/SiO_2 co-catalyst results in scavenging of photogenerated electrons by protons and water molecules, generating gaseous hydrogen and simultaneous oxidation of ethanol to acetaldehyde by photogenerated holes according to established radical chain reactions [41] or spillover mechanisms [42,43]. Controlled tests with only co-catalysts showed no generation of hydrogen from alcohol–water mixture in the wide range of temperatures (up to 60 °C). The nanoparticles of rutile show highest activity in the reaction of photogeneration of hydrogen (see Fig. 7) indicating the practical importance of such unusual material.

4. Conclusion

The treatment of titanate nanotubes with diluted sulphuric acid results in their transformation to TiO_2 nanostructures, the morphology and crystal phase of which depend on duration and temperature of the treatment. The decrease in temperature decelerates the transformation leading to formation of rutile nanoparticles. The transformation at elevated temperatures usually leads to rapid formation of anatase nanoparticles.

Nanostructured TiO_2 (both rutile and anatase) obtained via an acid route are characterized by a reduced adsorption constant (K^{E}_{ads}) and surface coverage (a_{sat}) for ethanol vapour at room temperature. Such a decrease in affinity towards ethanol is tentatively associated with modification of the surface nature rather than specific surface area (BET), which remains approximately unchanged during acid transformation of titanate nanotubes.

Studies of photocatalytic activity of TiO_2 nanostructures have shown that rutile nanoparticles obtained after 90 days of treatment titanate nanotubes with 0.1 mol dm^{-3} H_2SO_4 at 25 °C are characterized by higher activity in the reaction of hydrogen generation and similar activity in the reaction of ethanol oxidation as compared to standard P25. Such unusually high photocatalytic activity of rutile nanoparticles is probably connected with the unusual reduced temperature of their synthesis positively affecting the nature of the photocatalyst surface.

This preliminary photocatalytic studies suggest that acid treatment of titanate nanotubes can be considered as perspective route for preparation of photoactive nanostructured mix phase TiO_2.

Acknowledgements

The authors gratefully acknowledge financial support from the EPSRC, UK (grant EP/F044445/1) and NATO Collaborative Linkage Grant (CBP.NUKR.CLG 983748).

References

[1] A. Fujishima, K. Hashimoto, T. Watanabe, TiO_2 Photocatalysis: Fundamentals and Applications, BKC, USA, 1999.
[2] D.V. Bavykin, F.C. Walsh, Titanate and titania nanotubes: synthesis, properties and applications, RSC Nanosci. Nanotechnol. 2010.
[3] T. Kasuga, M. Hiramatsu, A. Hoson, T. Sekino, K. Niihara, Langmuir 14 (1998) 3160–3163.
[4] X. Chen, S.S. Mao, Chem. Rev. 107 (2007) 2891–2959.
[5] D.V. Bavykin, J.M. Friedrich, F.C. Walsh, Adv. Mater. 18 (2006) 2807–2824.
[6] Q. Chen, L.-M. Peng, Int. J. Nanotechnol. 4 (2007) 44–65.
[7] D.V. Bavykin, F.C. Walsh, Eur. J. Inorg. Chem. 8 (2009) 977–997.
[8] D.V. Bavykin, A.A. Lapkin, P.K. Plucinski, J.M. Friedrich, F.C. Walsh, J. Catal. 235 (2005) 10–17.
[9] V. Idakiev, Z.Y. Yuan, T. Tabakova, B.L. Su, Appl. Catal. A 281 (2005) 149–155.
[10] J. Yu, H. Yu, B. Cheng, X. Zhao, Q. Zhang, Q.J. Photochem, Photobiol. A: Chem. 182 (2006) 121–127.
[11] H. Langhuang, S. Zhongxin, L. Yingliang, J. Ceram. Soc. Jpn. 115 (2007) 28–31.
[12] X. Sun, Y. Li, Chem. Eur. J. 9 (2003) 2229–2238.
[13] D.V. Bavykin, F.C. Walsh, J. Phys. Chem. C 111 (2007) 14644–14651.
[14] A.R. Armstrong, G. Armstrong, J. Canales, P.G. Bruce, J. Power Sources 146 (2005) 501–506.
[15] F. Cheng, J. Chen, J. Mater. Res. 21 (2006) 2744–2757.
[16] Y. Ohsaki, N. Masaki, T. Kitamura, Y. Wada, T. Okamoto, T. Sekino, K. Niiharab, S. Yanagida, Phys. Chem. Chem. Phys. 7 (2005) 4157–4163.
[17] P.T. Hsiao, K.P. Wang, C.W. Cheng, H. Teng, J. Photochem. Photobiol. A: Chem. 188 (2007) 19–24.
[18] T. Tachikawa, S. Tojo, M. Fujitzuka, T. Sekino, T. Majima, J. Phys. Chem. B 110 (2006) 14055–14059.
[19] H.H. Ou, C.H. Liao, Y.H. Liou, J.H. Hong, S.L. Lo, Environ. Sci. Technol. 42 (2008) 4507–4512.
[20] G.S. Guo, C.N. He, Z.H. Wang, F.B. Gu, D.M. Han, Talanta 72 (2007) 1687–1692.
[21] M. Grandcolas, A. Louvet, N. Keller, V. Keller, Angew. Chem. Int. Ed. 48 (2009) 161–164.
[22] D.V. Bavykin, M. Carravetta, A.N. Kulak, F.C. Walsh, Chem. Mater. 22 (2010) 2458–2465.
[23] E. Morgado Jr., P.M. Jardim, B.A. Marinkovic, F.C. Rizzo, M.A.S. Abreu1, J.L. Zotin, A.S. Araujo, Nanotechnology 18 (2007) 495710–495810.
[24] J. Yu, H. Yu, B. Cheng, C. Trapalis, J. Mol. Catal. A 249 (2006) 135–142.
[25] Z. Gao, S. Yang, C. Sun, J. Hong, Sep. Purif. Technol. 58 (2007) 24–31.
[26] H.Y. Zhu, Y. Lan, X.P. Gao, S.P. Ringer, Z.F. Zheng, D.Y. Song, J.C. Zhao, J. Am. Chem. Soc. 127 (2005) 6730–6736.
[27] D.V. Bavykin, J.M. Friedrich, A.A. Lapkin, F.C. Walsh, Chem. Mater. 18 (2006) 1124–1129.
[28] J. Yu, H. Yu, B. Cheng, X. Zhao, Q. Zhang, J. Photochem. Photobiol. A: Chem. 182 (2006) 121–127.
[29] Y. Yu, D. Xu, Appl. Catal. B 73 (2007) 166–171.
[30] D.V. Bavykin, B.A. Cressey, M.E. Light, F.C. Walsh, Nanotechnology 19 (2008) 275604–275605.
[31] S. Kuchmiy Ya, S.V. Kulik, A.I. Kryukov, Theor. Exp. Chem. 25 (1989) 509–514.
[32] G. Li, S. Ciston, Z.V. Saponjic, L. Chen, N.M. Dimitrijevic, T. Rajh, K.A. Gray, J. Catal. 253 (2008) 105–110.
[33] H.L. Kuo, C.Y. Kuo, C.H. Liu, J.H. Chao, C.H. Lina, Catal. Lett. 113 (2007) 7–12.
[34] J.N. Nian, H. Teng, J. Phys. Chem. B 110 (2006) 4193–4198.

[35] D.V. Kozlov, D.V. Bavykin, E.N. Savinov, Catal. Lett. 86 (2003) 169–172.
[36] Q. Chen, G.H. Du, S. Zhang, L.M. Peng, Acta Crystallogr. B: Struct. Sci. 58 (2002) 587–593.
[37] D.S. Muggli, J.T. McCue, J.L. Falconer, J. Catal. 173 (1998) 470–483.
[38] M.R. Nimlos, E.J. Wolfrum, M.L. Brewer, J.A. Fennell, G. Bintner, Environ. Sci. Technol. 30 (1996) 3102–3110.
[39] M.L. Sauer, D.F. Ollis, J. Catal. 158 (1996) 570–582.
[40] J. Cunningham, G. Al-Sayyed, J. Chem. Soc., Faraday Trans. 86 (1990) 3935–3941.
[41] K. Ikeda, H. Sakai, R. Baba, K. Hashimoto, A. Fujishima, J. Phys. Chem. B 101 (1997) 2617–2620.
[42] M.C. Blount, J.A. Buchholz, J.L. Falconer, J. Catal. 197 (2001) 303–314.
[43] A.V. Korzhak, N.I. Ermokhina, A.L. Stroyuk, V.K. Bukhtiyarov, A.E. Raevskaya, V.I. Litvin, S. Kuchmiy Ya, V.G. Ilyin, P.A. Manorik, J. Photochem. Photobiol. A 198 (2–3) (2008) 126–134.